

Triphenylantimony(V) Catecholates Based on *o*-Quinones, Derivatives of Benzo[*b*][1,4]-Dioxines and Benzo[*b*][1,4]-Dioxepines

A. I. Poddel'skii^a, *^a, L. S. Okhlopkova^a, I. N. Meshcheryakova^a, N. O. Druzhkov^a,
I. V. Smolyaninov^b, and G. K. Fukin^a

^aRazuvaev Institute of Organometallic Chemistry, Russian Academy of Sciences, Nizhny Novgorod, 603600 Russia

^bSouthern Research Center, Russian Academy of Sciences, Rostov-on-Don, 344006 Russia

*e-mail: aip@iomc.ras.ru

Received May 8, 2018; Revised June 15, 2018; Accepted August 24, 2018

Abstract—New catecholate complexes of triphenylantimony(V), (Etgly-3,6-DBCat)SbPh₃ (**I**), (Propgly-3,6-DBCat)SbPh₃ (**II**), and (Cat-3,6-DBCat)SbPh₃ (**III**), based on analogs of sterically hindered 3,6-di-*tert*-butyl-*o*-benzoquinone, 5,8-di-*tert*-butyl-2,3-dihydrobenzo[*b*][1,4]dioxine-6,7-dione (L¹), 6,9-di-*tert*-butyl-2,3-dihydrobenzo[*b*][1,4]dioxepine-7,8-dione (L²), and 1,4-di-*tert*-butyl-dibenzo[*b,e*][1,4]dioxine-2,3-dione (L³), which are the 2,3-dihydrobenzo[*b*][1,4]dioxine, 2,3-dihydrobenzo[*b*][1,4]dioxepine, and dibenzo[1,4]dioxine derivatives, respectively, have been synthesized. At room temperature catecholates **I** and **II** react with molecular oxygen adding an O₂ molecule to form the corresponding spiroendoperoxides **IV** and **V**. Catecholate **III** reacts with oxygen with the deep oxidation of the complex and formation of neutral *o*-benzoquinone. The molecular structures of complexes **I** and **III** are determined by X-ray diffraction analysis (CIF files CCDC nos. 1840299 (**I** · toluene) and 1840300 (**III**)).

Keywords: redox-active ligand, antimony, quinone, molecular oxygen, X-ray diffraction analysis, cyclic voltammetry

DOI: 10.1134/S1070328419010093

INTRODUCTION

The reversible addition of molecular oxygen to triphenylantimony(V) catecholates and *o*-amidophenolates is one of interesting examples of the unusual chemical behavior of complexes of the main group metals related to the presence of a redox-active ligand of the *o*-quinone type in the metal complex [1–5]. As shown earlier, triphenylantimony(V) 4-methoxy- and 4,5-dimethoxy-3,6-di-*tert*-butylcatecholates are characterized by the highest reactivity toward oxygen among the triphenylantimony(V) catecholates [5–7]. Their reactivity is caused by the presence of the strong electron-donor methoxy substituents in the 3,6-di-*tert*-butylcatecholate ligand [7, 8]. The related catecholate complexes of antimony(V), (Etgly-3,6-DBCat)SbPh₃ (**I**), (Propgly-3,6-DBCat)SbPh₃ (**II**), and (Cat-3,6-DBCat)SbPh₃ (**III**), which are the derivatives of dioxines and dioxepines (Scheme 1), should exhibit similar properties. The results of studying the structures and some physicochemical properties of the new triphenylantimony(V) complexes are presented in this work.

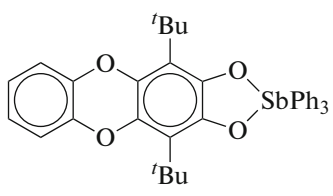
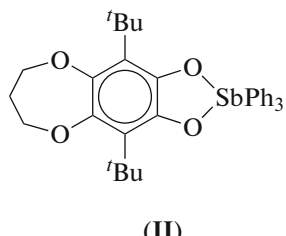
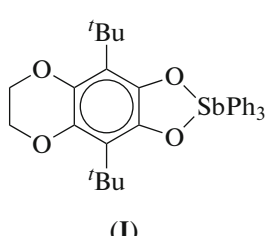
RESULTS AND DISCUSSION

The introduction of ethylene- and propyleneglycol groups into 3,6-di-*tert*-butyl-*o*-benzoquinone leads to the formation of new *o*-benzoquinones functionalized by the electron-donor groups (5,8-di-*tert*-butyl-2,3-dihydrobenzo[*b*][1,4]dioxine-6,7-dione (L¹) and 6,9-di-*tert*-butyl-2,3-dihydro-2*H*-benzo[*b*][1,4]di-oxepine-7,8-dione (L²)) [9, 10]. 1,4-Di-*tert*-butyldibenzo[*b,e*][1,4]dioxine-2,3-dione (L³) (dibenzo[1,4]dioxine derivative) was first obtained in this work by the reaction of 3,6-di-*tert*-butyl-*o*-benzoquinone (3,6-Q) with pyrocatechol under alkaline catalysis conditions.

Catecholate derivatives of triphenylantimony(V) **I**–**III** (Scheme 1) are synthesized by the oxidative addition of these *o*-benzoquinones to triphenylantimony. The oxidation of triphenylstibine by these *o*-benzoquinones is slower than, for example, the oxidation by 3,6-di-*tert*-butyl-*o*-benzoquinone.

Table 1. Selected bond lengths (d) and bond angles (ω) in complexes **I** and **III**

Bond	<i>d</i> , Å		Bond	<i>d</i> , Å	
	I	III		I	III
Sb(1)–O(1)	2.0030(11)	2.0174(7)	O(4)–C(8)	1.433(2)	1.3753(13)
Sb(1)–O(2)	2.0271(11)	2.0201(8)	C(1)–C(2)	1.414(2)	1.4174(13)
Sb(1)–C(17)	2.1398(17)		C(1)–C(6)	1.397(2)	1.3961(13)
Sb(1)–C(21)		2.1379(11)	C(2)–C(3)	1.398(2)	1.4002(14)
Sb(1)–C(23)	2.1464(17)		C(3)–C(4)	1.412(2)	1.4069(15)
Sb(1)–C(27)		2.1308(11)	C(4)–C(5)	1.388(2)	1.3877(14)
Sb(1)–C(29)	2.1032(16)		C(5)–C(6)	1.415(2)	1.4055(14)
Sb(1)–C(33)		2.1024(10)	C(7)–C(8)	1.501(3)	1.3849(17)
O(1)–C(1)	1.3646(19)	1.3534(12)	C(7)–C(12)		1.3840(16)
O(2)–C(2)	1.3722(19)	1.3592(12)	C(8)–C(9)		1.3829(16)
C(4)–O(3)	1.3942(19)	1.3947(13)	C(9)–C(10)		1.3951(18)
C(5)–O(4)	1.3885(19)	1.3985(13)	C(10)–C(11)		1.382(2)
O(3)–C(7)	1.421(2)	1.3735(15)	C(11)–C(12)		1.389(2)
Angle	ω , deg		Angle	ω , deg	
	I	III		I	III
O(1)Sb(1)O(2)	78.25(4)	78.07(3)	O(2)Sb(1)C(27)		146.77(4)
O(1)Sb(1)C(17)	151.05(5)		O(2)Sb(1)C(29)	103.11(5)	
O(1)Sb(1)C(21)		156.06(4)	O(2)Sb(1)C(33)		104.59(4)
O(1)Sb(1)C(23)	84.33(5)		C(17)Sb(1)C(23)	98.65(6)	
O(1)Sb(1)C(27)		84.19(4)	C(21)Sb(1)C(27)		100.50(4)
O(1)Sb(1)C(29)	100.76(5)		C(17)Sb(1)C(29)	106.32(6)	
O(1)Sb(1)C(33)		97.38(4)	C(21)Sb(1)C(33)		103.83(4)
O(2)Sb(1)C(17)	85.74(6)		C(23)Sb(1)C(29)	104.02(6)	
O(2)Sb(1)C(21)		85.86(4)	C(27)Sb(1)C(33)		105.39(4)
O(2)Sb(1)C(23)	150.00(5)				



Scheme 1.

Catecholates **I**–**III** were isolated in the individual form and characterized by IR spectroscopy, NMR spectroscopy, mass spectrometry, and elemental analysis.

The molecular structures of catecholates **I** and **III** in the crystalline state were determined by X-ray diffraction analysis (Fig. 1). The central antimony atoms in both complexes are in the distorted tetragonal pyramidal environment. The τ parameter used for the description of polyhedra with the coordination number 5 is 0.02 for compound **I** and 0.15 for compound **III** ($\tau = 1$ for an ideal trigonal bipyramid and $\tau = 0$ for an ideal tetragonal pyramid [11]). The lengths of the Sb(1)–C(29) bond in the apical phenyl group in compound **I** and Sb(1)–C(33) bond in compound **III** are shorter than the lengths of the Sb–C bonds in the phenyl groups in the pyramid base by 0.037–0.043 and 0.028–0.035 Å, respectively (Table 1). The geometric

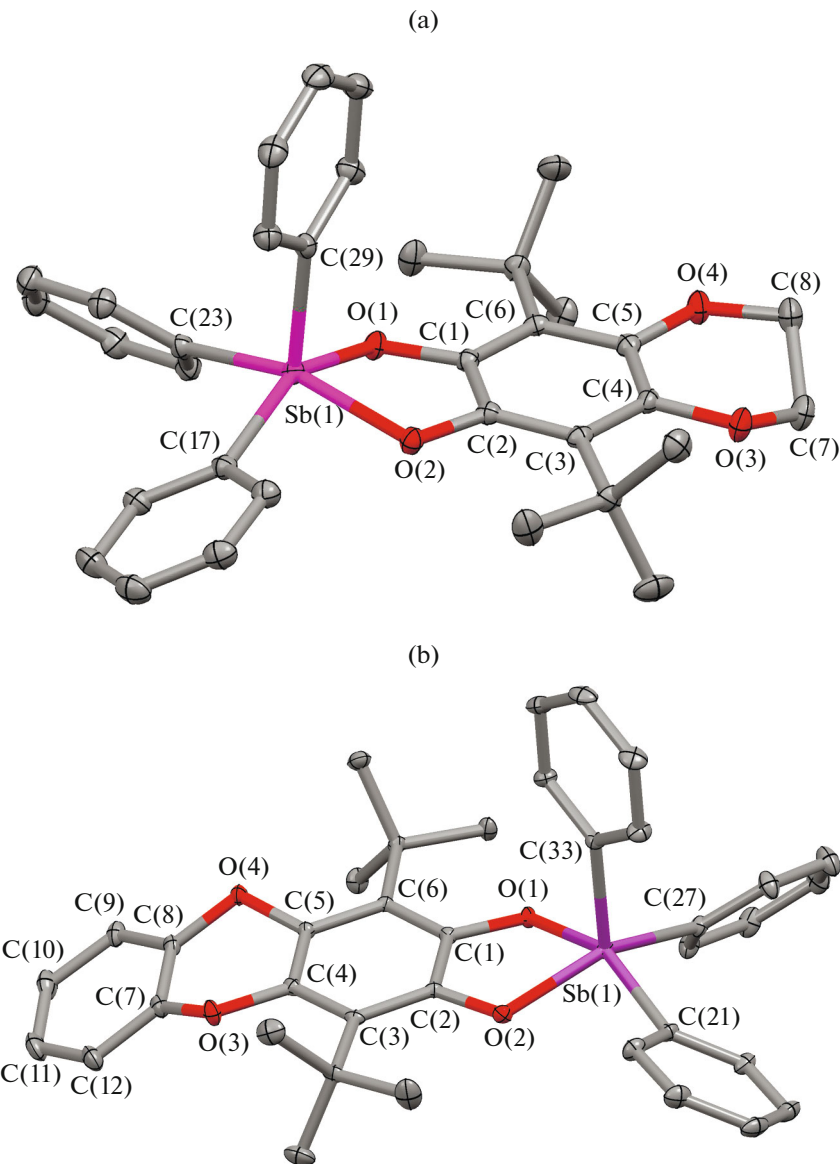


Fig. 1. Molecular structures of catecholates (a) I and (b) III. Hydrogen atoms are omitted; ellipsoids of 50% probability.

characteristics of the redox-active ligands (lengths of the C–O and C–C bonds of the six-membered ring of the redox-active ligand) in complexes **I** and **III** are close to the values of the earlier characterized catecholate complexes of triphenyl- [12–20], diphenylaryl-, phenyldiaryl- and triaryl- [21–30], and trialkylantimony(V) [31–33].

It seems interesting to describe specific features of the crystal packings of these complexes. In the crystal cell of complex **I**, the molecules are joined in chains in which the phenyl ring in the apical position of one molecule of the complex is directed nearly to the center of the aromatic ring of the catecholate ligand of the adjacent molecule (Fig. 2a). The distances between the C(32) and C(4)–C(6) atoms of the aromatic ring of the catecholate ligand of the adjacent molecule are

3.630(2), 3.655(2), and 3.765(2) Å, respectively, which exceeds the doubled van der Waals radius of carbon (3.4 Å [34]). The distances between the corresponding hydrogen atom H(32) and C(4)–C(6) atoms of the adjacent molecule are 2.75, 2.73, and 2.88 Å, respectively, and are comparable with the sum of the van der Waals radii of hydrogen and carbon atoms (2.9 Å [34]). In the crystals of complex **III**, the adjacent molecules are bound in pairs (Fig. 2b) and the apical phenyl rings of the molecules are directed nearly to the centers of the aromatic rings of the catecholate ligands. The distances between the C(36) atom of the phenyl group of one molecule and the C(3)–C(5) atoms of the catecholate ligand of the pair molecule are 3.732(2), 3.622(2), and 3.631(2) Å, respectively. The distances between the H(36) atom of

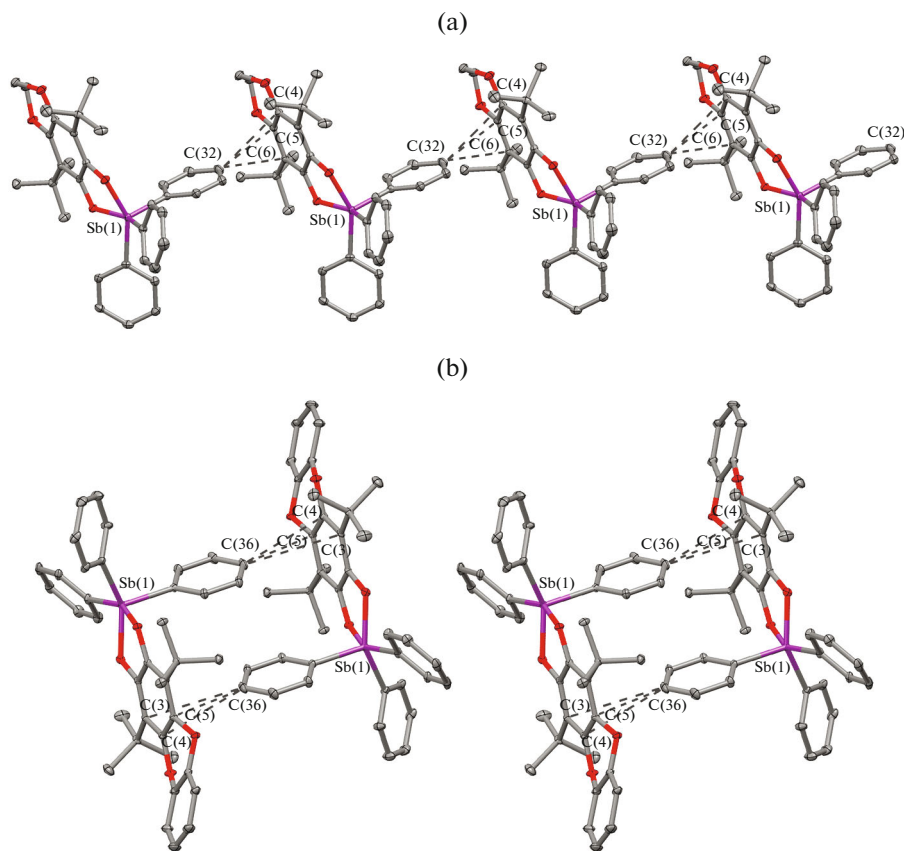


Fig. 2. Crystal packing fragments of complexes (a) **I** and (b) **III**. Hydrogen atoms are omitted; ellipsoids of 50% probability.

the C(36) atom of one molecule and these carbon atoms of the catecholate ligand of the adjacent molecule are 2.82, 2.70, and 2.7 Å, respectively. Thus, it can be assumed that the chain and dimeric motifs in compounds **I** and **III**, respectively, occur due to the H...π interactions.

The electrochemical behavior of catecholate complex **II** was studied by the CV method in a dichloromethane solution at the GC electrode under anaerobic conditions. Two oxidation steps at the potentials $E_{1/2}^1 = 0.65$ and $E_{pa}^2 = 0.99$ V corresponding to a change in the oxidation state of the coordinated catecholate ligand are detected in the CV curves of complex **II** (Fig. 3). The detected oxidation potentials are nearly identical to those obtained previously for the 4,5-dimethoxy-3,6-di-*tert*-butylcatecholate derivative of triphenylantimony(V) ($E_{1/2}^1 = 0.65$, $E_{pa}^2 = 1.08$ V) [7, 8]. The only distinction is the shift of the oxidation potential of the second peak to the cathodic region by 0.09 V.

The relatively stable ($I_c/I_a = 0.75$) within the CV experimental time monocationic complex $[(\text{Propgly-3,6-SQ})\text{SbPh}_3]^+$ is generated as a result of the first quasi-reversible one-electron process. The low stabil-

ity of the formed complex is confirmed by the appearance of the reduction peak (-0.69 V) in the reverse branch of the voltammogram. The peak belongs to the product of the chemical reaction following the electron transfer. The detected cathodic peak can be assigned to the reduction of decoordination *o*-benzoquinone. The second oxidation step is irreversible and leads to the formation of the unstable dication $[(\text{Propgly-3,6-BQ})\text{SbPh}_3]^{++}$, which decomposes to form free *o*-benzoquinone. The pulse potential scan results in the detection of the reduction peak of decoordination *o*-benzoquinone (Fig. 4).

The value of the oxidation potential of the first redox transition, $E_{1/2}^1 = 0.65$ V, assumes a possibility for the reaction with air oxygen to occur with the formation of the spiroendoperoxide complex [7, 35, 36]. The electrochemical pattern changes in the presence of air oxygen: the currents of two peaks decrease and a new anodic peak appears at 1.35 V (Fig. 5). A similar behavior was earlier detected for triphenylantimony(V) 4,5-dimethoxy-3,6-di-*tert*-butylcatecholate for which the oxidation peak of the spiroendoperoxide complex was observed at 1.28 V. The peaks of decoordination *o*-benzoquinone appear gradually in the CV

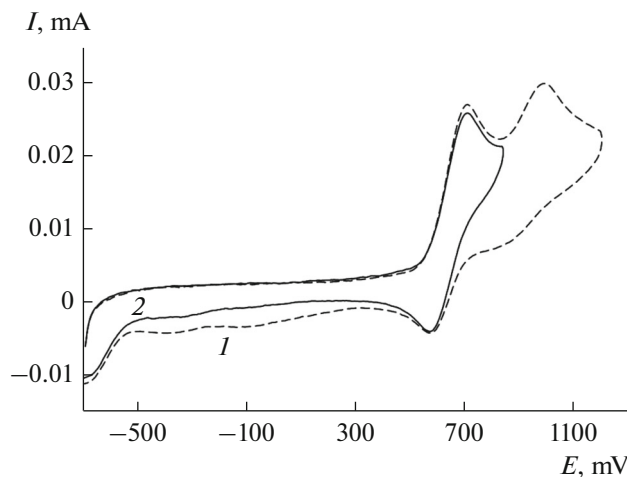


Fig. 3. Cyclic voltammograms for the oxidation of complex **II** in the potential scan range: (1) from -0.7 to 1.20 V and (2) from -0.7 to 0.85 V; CH_2Cl_2 , GC anode, 0.15 M Bu_4NClO_4 , $c = 0.002$ mol/L, $\text{Ag}/\text{AgCl}/\text{KCl}$ (sat.), Ar.

curve, indicating a low stability of the corresponding spiroendoperoxide under these conditions.

Indeed, catecholates **I**–**III** were found to be highly sensitive to air oxygen. The reactions of ethylene- and propyleneglycol-containing catecholates **I** and **II** with air oxygen afford the corresponding spiroendoperoxide derivatives **IV** and **V** (Scheme 2), which is seen from the changes observed in the NMR spectra of the complexes in the presence of air oxygen. However, the deeper oxidation occurs with time to liberate neutral *o*-benzoquinones (Scheme 2), which is confirmed by the data of NMR spectroscopy. The signals corresponding to free *o*-benzoquinones L^1 and L^2 appear

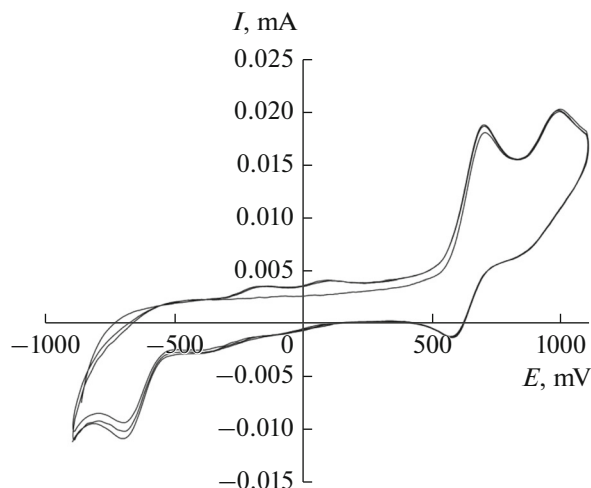
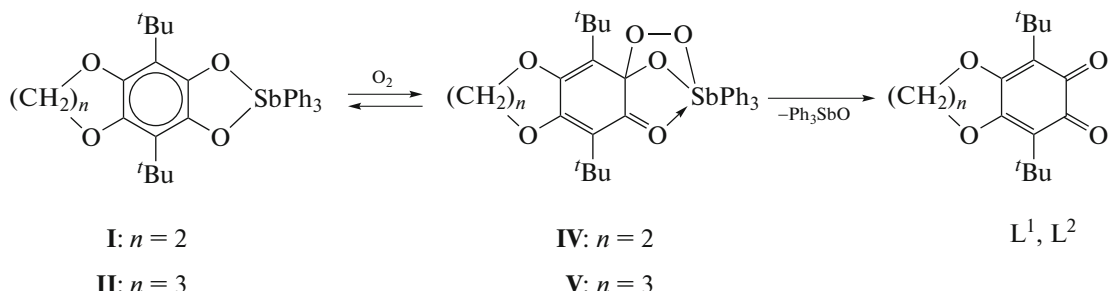


Fig. 4. Cyclic voltammograms for the oxidation of complex **II** in the pulse potential scan range from -0.9 to 1.1 V; CH_2Cl_2 , GC anode, 0.15 M Bu_4NClO_4 , $c = 0.0015$ mol/L, $\text{Ag}/\text{AgCl}/\text{KCl}$ (sat.), Ar.

gradually as solutions of the complexes are kept in air (singlets at 1.30 ppm from protons of the *tert*-butyl groups (in both *o*-benzoquinones) and a singlet at 4.35 ppm for ethyleneglycol-substituted *o*-benzoquinone or a quintuplet at 2.22 ppm and a triplet at 4.25 ppm from propyleneglycol-substituted *o*-benzoquinone). The obtained results are consistent with the electrochemical investigation data for complex **II** in air: the decoordination of the corresponding *o*-benzoquinone for this complex occurs more rapidly than that for the dimethoxy-substituted derivative. Free *o*-quinone L^3 is almost immediately formed upon the reaction of catecholate **III** with air oxygen.



Scheme 2.

To conclude, the new catecholate complexes of triphenyltantalum(V) containing the electron-donor ethyleneglycol, propyleneglycol, and *o*-phenylenediolate groups in positions 4 and 5 of the 3,6-di-*tert*-butylcatecholate ligand were synthesized from *o*-benzoquinones, the derivatives of 2,3-dihydrobenzo[*b*]-[1,4]dioxine, 2,3-dihydrobenzo[*b*][1,4]dioxepine,

and dibenzo[1,4]dioxine. At room temperature triphenyltantalum(V) catecholates react with molecular oxygen adding an O_2 molecule to form the corresponding spiroendoperoxides. However, these spiroendoperoxide derivatives are lowly stable, and the deeper oxidation occurs with time to liberate neutral *o*-benzoquinones.

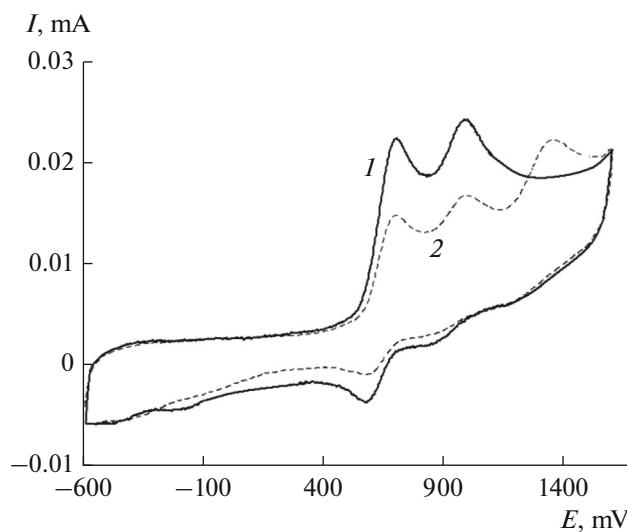


Fig. 5. Cyclic voltammograms for the oxidation of complex **II** in the potential scan range from -0.6 to 1.6 V: (1) anaerobic and (2) aerobic conditions; CH_2Cl_2 , GC anode, 0.15 M Bu_4NClO_4 , $c = 0.0015$ mol/L, $\text{Ag}/\text{AgCl}/\text{KCl}$ (sat.).

EXPERIMENTAL

The solvents used were purified and dehydrated by standard procedures [37]. *o*-Benzoquinones **L**¹ and **L**² were synthesized according to published procedures [9, 10]. The complexes were synthesized in evacuated tubes in the absence of oxygen and moisture.

¹H and ¹³C NMR spectra were recorded on a Bruker AVANCE DPX-200 spectrometer using tetramethylsilane as an internal standard and CDCl_3 as a solvent. IR spectra were measured on an FSN-1201 FT-IR spectrometer in Nujol in a range of 400 – 4000 cm^{-1} . Elemental analysis (C, H, Sb) was conducted using the pyrolytic method with gravimetric finishing.

The electrochemical potentials of the studied compounds were measured by cyclic voltammetry (CV) in a three-electrode cell on an IPC-pro potentiostat in dichloromethane or acetonitrile under argon. A stationary glassy carbon (GC) electrode with a diameter of 2 mm served as a working electrode, and a platinum plate ($S = 18$ mm^2) was used as an auxiliary electrode. An $\text{Ag}/\text{AgCl}/\text{KCl}$ reference electrode with a water-impervious membrane was used. The concentration of complex **II** was 0.0030 – 0.0015 mol/L. The number of electrons transferred during the electrode process was estimated relative to ferrocene used as a standard. The potential scan rate was 0.2 V s^{-1} (0.1 M Bu_4NClO_4 (99%, Acros) as a supporting electrolyte).

X-ray diffraction analyses of the complexes were carried out on Bruker Smart Apex I (**I**·toluene) and Bruker D8 Quest CMOS (**III**) diffractometers at 100 K. The structures were determined by a direct method and refined by full-matrix least squares for

F_{hkl}^2 in the anisotropic approximation for all non-hydrogen atoms. Hydrogen atoms were placed in the geometrically calculated positions and refined isotropically. The calculations were performed using the SHELXTL program package [38]. An absorption correction was applied using the SADABS program [39]. The crystallographic data and the parameters of X-ray diffraction experiments and refinement for **I**·toluene and **III** are presented in Table 2. The structural data were deposited with the Cambridge Crystallographic Data Centre (CIF files CCDC nos. 1840299 (**I**·toluene) and 1840300 (**III**); deposit@ccdc.cam.ac.uk; <http://www.ccdc.cam.ac.uk>).

Synthesis of **L³.** Pyrocatechol (0.5 g, 4.5 mmol), NaOH (0.018 g, 0.45 mmol (10 mol %)), and MnO_2 (0.1 g, 1.15 mmol (25 mol %)) were added to a solution of **3,6-Q** (1 g, 4.5 mmol) in DMF (30 mL). The obtained reaction mixture was heated at 50°C with stirring for 6 h. The color of the solution changed from green-vinous to red-orange. The reaction course was monitored by the TLC method. In 6 h, pyrocatechol (1 g, 9 mmol) was added by portions to the reaction mixture with permanent stirring until no unreacted **3,6-Q** remained in the system (according to TLC). Then the reaction mixture was filtered through a paper folded filter. Water was added dropwise with stirring to the obtained solution in order to precipitate **L**³. The precipitated product was collected on a glass Schott filter no. 4 and dried in air. The yield of analytically pure product **L**³ was 0.44 g (30%).

For $\text{C}_{20}\text{H}_{22}\text{O}_4$

Anal. calcd., %	C, 73.60	H, 6.79
Found, %	C, 73.57	H, 6.81

IR (ν , cm^{-1}): 1671 s, 1664 s, 1650 m, 1633 m, 1624 s, 1574 m, 1556 s, 1537 m, 1497 s, 1480 s, 1414 w, 1397 m, 1365 m, 1324 s, 1308 s, 1295 s, 1201 m, 1171 w, 1154 w, 1108 w, 1053 w, 1034 w, 977 m, 939 w, 931 w, 903 w, 818 w, 805 w, 779 w, 761 s, 647 w, 595 w, 563 w. ¹H NMR (CDCl_3 ; δ , ppm): 1.48 (s, 18H , *t*-Bu), 7.13 – 7.24 (m, 4H , arom., C_6H_4). ¹³C NMR (CDCl_3 ; δ , ppm): 30.45 , 35.85 , 116.28 , 124.83 , 127.49 , 137.84 , 149.38 , 183.02 .

Synthesis of 4,5-(ethane-1,2-diolato)-3,6-di-*tert*-butylcatecholato)triphenylantimony(V**) (**I**).** Solutions of triphenylantimony (0.0843 g, 0.24 mmol) and **L**¹ (0.0664 g, 0.24 mmol) were mixed in a toluene solution at room temperature. The color gradually changed from green to yellow as the reactants were mixed. After the completion of the reaction, toluene was removed under reduced pressure and the residue was dissolved in hexane. The obtained solution was

Table 2. Crystallographic data and the experimental and refinement characteristics for compounds **I** · toluene and **III**

Parameter	Value	
	I · toluene	III
<i>FW</i>	723.52	679.42
<i>T</i> , K	150(2)	100(2)
Crystal system	Monoclinic	Triclinic
Space group	<i>P</i> 2 ₁ / <i>c</i>	<i>P</i> 1̄
Cell parameters:		
<i>a</i> , Å	15.8733(6)	11.4757(5)
<i>b</i> , Å	9.7467(4)	11.6202(5)
<i>c</i> , Å	22.5386(9)	14.0014(6)
α, deg	90	80.1740(10)
β, deg	97.6800(10)	79.5290(10)
γ, deg	90	60.8220(10)
<i>V</i> , Å ³	3455.7(2)	1595.69(12)
<i>Z</i>	4	2
ρ _{calcd.} , g/cm ³	1.391	1.414
μ, mm ⁻¹	0.839	0.904
<i>F</i> (000)	1496	696
2θ _{max} , deg	52	74.07
Number of measured reflections	20380	35330
Number of independent reflections	6728	16159
<i>R</i> _{int}	0.0231	0.0228
Number of refined parameters	422	394
<i>R</i> ₁ , <i>wR</i> ₂ (<i>I</i> > 2σ(<i>I</i>))	0.0269, 0.0652	0.0277, 0.0665
<i>R</i> ₁ , <i>wR</i> ₂ (for all data)	0.0323, 0.0675	0.0332, 0.0685
GOOF for <i>F</i> ²	1.059	1.062
Residual electron density (max/min), e/Å ³	1.067/-0.278	1.288/-0.527

left to stay for 2 days at -15°C. Complex **I** was isolated from hexane as orange crystals. The yield was 88%.

For C₃₄H₃₇O₄Sb

Anal. calcd., % C, 64.67 H, 5.91 Sb, 19.28
Found, % C, 65.08 H, 6.09 Sb, 18.79

IR (Nujol; ν, cm⁻¹): 1578 m, 1528 s, 1478 m, 1433 m, 1405 s, 1367 m, 1349 s, 1306 s, 1250 m, 1207 m, 1173 m, 1156 w, 1127 m, 1100 s, 1072 m, 1019 m, 998 m, 970 m, 954 m, 927 w, 916 w, 895 m, 848 w, 802 w, 782 w, 772 m, 738 m, 731 s, 694 s, 675 m, 661 w, 588 w, 581 w, 568 w, 550 w, 518 w, 509 w, 499 w, 480 w, 461 m, 450 m, 439 w, 427 w, 417 m, 403 m. ¹H NMR (CDCl₃; δ, ppm): 1.52 (s, 18 H, *t*-Bu), 4.11 (s, 4 H, -CH₂CH₂-), 7.36–7.50 (m, 9 H, arom., SbPh₃), 7.67–7.76 (m, 6 H, arom., SbPh₃). EI-MS (*m/z*): 630, 632 ([M]⁺).

Synthesis of (4,5-(propane-1,3-diolato)-3,6-di-*tert*-butylcatecholato)triphenylantimony(V) (II) was carried out by the reaction of triphenylantimony (0.0882 g, 0.25 mmol) and L² (0.073 g, 0.25 mmol) using the method similar to that for complex **I**. The yield of a yellow-orange powder of complex **II** was 91%.

For C₃₅H₃₉O₄Sb

Anal. calcd., % C, 65.13 H, 6.09 Sb, 18.86
Found, % C, 65.27 H, 6.34 Sb, 18.50

IR (Nujol, cm⁻¹): 1570 m, 1530 s, 1471 m, 1429 m, 1395 s, 1360 m, 1329 s, 1311 m, 1242 m, 1201 m, 1165 m, 1150 w, 1127 m, 1105 s, 1077 m, 1023 w, 995 m, 965 m, 952 w, 923 w, 910 w, 891 m, 847 w, 785 w, 774 s, 735 m, 730 s, 691 s, 673 w, 657 w, 580 w, 571 w, 540 w, 520 w, 496 w, 477 w, 460 m, 450 m, 441 w, 419 w, 405 m. ¹H NMR (CDCl₃; δ, ppm): 1.53 (s, 18 H,

t-Bu), 2.04 (quint, $^3J(\text{H},\text{H}) = 5.0$ Hz, 2 H, $-\text{CH}_2\text{CH}_2\text{CH}_2-$), 3.90 (t, $^3J(\text{H},\text{H}) = 5.0$ Hz, 4 H, $-\text{CH}_2\text{CH}_2\text{CH}_2-$), 7.38–7.52 (m, 9 H, arom., SbPh_3), 7.67–7.78 (m, 6 H, arom., SbPh_3). EI-MS (m/z): 644, 646 ($[\text{M}]^+$).

Synthesis of (4,5-(phenylene-1,2-diolato)-3,6-di-*tert*-butylcatecholato)triphenylantimony(V) (III) was carried out by the reaction of L^3 (0.163 g, 0.5 mmol) and triphenylantimony (0.177 g, 0.5 mmol) using the method similar to that for complex I. The yield of an orange powder of compound III was 80%.

For $\text{C}_{38}\text{H}_{37}\text{O}_4\text{Sb}$

Anal. calcd., %	C, 67.17	H, 5.49	Sb, 17.92
Found, %	C, 67.28	H, 5.60	Sb, 17.69

^1H NMR (CDCl_3 ; δ , ppm): 1.62 (s, 18 H, *t*-Bu), 6.90 (br.s, 4 H, arom., C_6H_4), 7.40–7.62 (m, 9 H, arom., SbPh_3), 7.66–7.82 (m, 6 H, arom., SbPh_3).

^{13}C NMR (CDCl_3 ; δ , ppm): 31.99, 36.34, 115.43, 120.13, 122.87, 129.14, 131.09, 134.90, 136.25, 137.79, 141.54, 145.14. EI-MS (m/z): 678, 680 ($[\text{M}]^+$).

Syntheses of 4,5-(ethane-1,2-diolato)-2-oxo-3,6-di-*tert*-butylcyclohexa-3,5-diene-1-peroxo-1-olato-O, O',O'")triphenylantimony(V) [(Etgly-L)(O₂)-SbPh₃] (IV) and 4,5-(propane-1,3-diolato)-2-oxo-3,6-di-*tert*-butylcyclohexa-3,5-diene-1-peroxo-1-olato-O',O'") triphenylantimony(V) [(Propgly-L)(O₂-SbPh₃)] (V) were carried out by the dissolution of the corresponding initial catecholates I and II in deuterated chloroform in air and keeping the obtained solution for several hours.

^1H NMR (CDCl_3 ; δ , ppm) for IV: 1.29 (br.s, 18 H, *t*-Bu), 4.28 (s, 4 H, O-CH₂-CH₂-O), 7.30–7.80 (m, 15 H, arom., SbPh_3).

^1H NMR (CDCl_3 ; δ , ppm) for V: 1.29 (br.s, 18 H, *t*-Bu), 2.19 (m, 2 H, O-CH₂-CH₂-CH₂-O), 4.21 (m, 4 H, O-CH₂-CH₂-CH₂-O), 7.30–7.80 (m, 15 H, arom., SbPh_3).

ACKNOWLEDGMENTS

This work was carried out using the scientific equipment of the Center for Collective Use “Analytical Center of the Razuvayev Institute of Organometallic Chemistry of the Russian Academy of Sciences.” The X-ray diffraction studies of the complexes were conducted in terms of the state task (theme no. 44.2, registration no. AAAA-A16-116122110053-1).

This work was supported by the Russian Foundation for Basic Research, project no. 16-33-60157 mol_a_dk.

REFERENCES

1. Abakumov, G.A., Poddel'sky, A.I., Grunova, E.V., et al., *Angew. Chem., Int. Ed. Engl.*, 2005, vol. 44, p. 2767.
2. Cherkasov, V.K., Abakumov, G.A., Grunova, E.V., et al., *Chem.-Eur. J.*, 2006, vol. 12, no. 14, p. 3916.
3. Poddel'sky, A.I., Kurskii, Yu.A., Piskunov, A.V., et al., *Appl. Organomet. Chem.*, 2011, vol. 25, no. 3, p. 180.
4. Fukin, G.K., Baranov, E.V., Jelsch, C., et al., *J. Phys. Chem. A*, 2011, vol. 115, no. 29, p. 8271.
5. Abakumov, G.A., Cherkasov, V.K., Grunova, E.V., et al., *Dokl. Akad. Nauk.*, 2005, vol. 405, no. 2, p. 199.
6. Poddel'sky, A.I., Smolyaninov, I.V., Kurskii, Yu.A., et al., *Izv. Akad. Nauk., Ser. Khim.*, 2009, no 3, p. 520.
7. Smolyaninov, I.V., Poddel'skiy, A.I., Berberova, N.T., et al., *Russ. J. Coord. Chem.*, 2010, vol. 36, p. 644. doi 10.1134/S1070328410090022
8. Smolyaninov I.V., Poddel'skiy A.I., Smolyaninova S.A., et al., *Russ. J. Gen. Chem.*, 2014, vol. 84, no. 9, p. 1761.
9. Prokof'eva, T.I., Vol'eva, V.B., Prokof'ev, A.I., et al., *Khim. Geterotsikl. Soed.*, 2000, vol. 36, no. 8, p. 1057.
10. Shurygina, M.P., Druzhkov, N.O., Arsen'ev, M.V., et al., *Zh. Org. Khim.*, 2011, vol. 47, no. 4, p. 490.
11. Addison, A.W., Rao, T.N., Reedijk, J., et al., *J. Chem. Soc., Dalton Trans.* (1972–1999), 1984, p. 1349.
12. Hall, M. and Sowerby, D.B., *J. Am. Chem. Soc.*, 1980, vol. 102, p. 628.
13. Holmes, R.R., Day, R.O., Chandrasekhar, V., et al., *Inorg. Chem.*, 1987, vol. 26, p. 163.
14. Poddel'sky, A.I., Baranov, E.V., Fukin, G.K., et al., *J. Organomet. Chem.*, 2013, vol. 733, p. 44.
15. Poddel'sky, A.I., Ilyakina, E.V., Smolyaninov, I.V., et al., *Izv. Akad. Nauk. Ser. Khim.*, 2014, no. 4, p. 923.
16. Protasenko, N.A., Poddel'skiy, A.I., Smolyaninov, I.V., et al., *Izv. Akad. Nauk. Ser. Khim.*, 2014, no. 4, p. 930.
17. Poddel'sky, A.I., Smolyaninov, I.V., Fukin, G.K., et al., *J. Organomet. Chem.*, 2016, vol. 824, p. 1.
18. Poddel'sky, A.I., Arsenyev, M.V., Astaf'eva, T.V., et al., *J. Organomet. Chem.*, 2017, vol. 835, p. 17.
19. Poddel'sky, A.I., Arsen'ev, M.V., Okhlopkova, L.S., et al., *Russ. J. Coord. Chem.*, 2017, vol. 43, p. 843. doi 10.1134/S1070328417120089
20. Arsen'ev, M.V., Okhlopkova, L.S., Poddel'skiy, A.I., et al., *Russ. J. Coord. Chem.*, 2018, vol. 44, p. 162. doi 10.1134/S1070328418020021
21. Holmes, R.R., Day, R.O., Chandrasekhar, V., et al., *Inorg. Chem.*, 1987, vol. 26, p. 157.
22. Fukin, G.K., Baranov, E.V., Poddelskiy, A.I., et al., *ChemPhysChem*, 2012, vol. 13, p. 3773.
23. Ke, I.-Sh. and Gabbai, F.P., *Inorg. Chem.*, 2013, vol. 52, p. 7145.
24. Jones, J.S., Wade, C.R., and Gabbai, F.P., *Angew. Chem., Int. Ed. Engl.*, 2014, vol. 53, p. 8876.
25. Hirai, M. and Gabbai, F.P., *Chem. Sci.*, 2014, vol. 5, p. 1886.

26. Poddel'sky, A.I., Smolyaninov, I.V., Berberova, N.T., et al., *J. Organomet. Chem.*, 2015, vols. 789–790, p. 8.
27. Hirai, M. and Gabbai, F.P., *Angew. Chem., Int. Ed. Engl.*, 2015, vol. 54, p. 1205.
28. Tofan, D. and Gabbai, F.P., *Chem. Sci.*, 2016, vol. 7, p. 6768.
29. Poddel'sky, A.I., Druzhkov, N.O., Fukin, G.K., et al., *Polyhedron*, 2017, vol. 124, p. 41.
30. Chen, C.-H. and Gabbai, F.P., *Angew. Chem., Int. Ed. Engl.*, 2017, vol. 56, p. 1799.
31. Fukin, G.K., Zakharov L.N., Domrachev G.A., et al., *Izv. Akad. Nauk, Ser. Khim.*, 1999, p. 1744.
32. Poddel'sky, A.I., Somov, N.V., Druzhkov, N.O., et al., *J. Organomet. Chem.*, 2011, vol. 696, p. 517.
33. Poddel'sky, A.I., Smolyaninov, I.V., Fukin, G.K., et al., *J. Organomet. Chem.*, 2018, vol. 867, p. 238.
34. Batsanov, S.S., *Zh. Neorg. Khim.*, 1991, vol. 36, no. 12, p. 3015.
35. Poddel'sky, A.I., Smolyaninov, I.V., Kurskii, Y.A., et al., *J. Organomet. Chem.*, 2010, vol. 695, no. 8, p. 1215.
36. Smolyaninova, S.A., Poddel'sky, A.I., Smolyaninov, I.V., et al., *Russ. J. Coord. Chem.*, 2014, vol. 40, p. 273. doi 10.1134/S107032841405011X
37. Gordon, A. and Ford, R., *The Chemist's Companion: A Handbook of Practical Data, Techniques, and References*, New York: Wiley, 1972.
38. Sheldrick, G.M., *SHELXTL. Version 6.14. Structure Determination Software Suite*, Madison: Bruker AXS, 2003.
39. Sheldrick, G.M., *SADABS. Version 2012/1. Bruker/Siemens Area Detector Absorption Correction Program*, Madison: Bruker AXS, 2012.

Translated by E. Yablonskaya